COBEM 2021 26th International Congress of Mechanical Engineering
November 22-26, 2021, Virtual Congress, Brazil

COB-2021-0929
COMPARISON OF THE THERMAL EFFICIENCY OF A GAS TURBINE WORKING WITH COMBUSTION AND DETONATION CHAMBERS

Ramiro Veronese de Vargas
Universidade Federal do Rio Grande do Sul, Rua Sarmento Leite, 425
ramiro_veronese@hotmail.com
Rodrigo Savi Justi
Universidade Federal do Rio Grande do Sul, Rua Sarmento Leite, 425
rodrigo.justi@ufrgs.br
César A. Quispe Gonzáles
Universidad Nacional Mayor de San Marcos, Lima District 15081, Peru
cquispeg@unmsm.edu.pe
Andrés A. Mendiburu Zevallos
Universidade Federal do Rio Grande do Sul, Rua Sarmento Leite, 425
International Research Group for Energy Sustainability (IRGES)
andresmendiburu@ufrgs.br

Abstract. *The objective of the present study is to perform a thermodynamic comparison of the thermal efficiency by varying the main parameters of a power generation cycle involving gas turbines, where the combustion products are obtained in two different processes: by constant-pressure combustion inside a conventional combustion chamber and by a detonation process inside a detonation chamber. To achieve this goal, a study of combustion reactions in the context of equilibrium thermodynamics was performed; then, a computational model was developed in order to study the aforementioned processes. The thermodynamic model allows to study the influence of the compression ratio, fuel composition and equivalence ratio on the thermal efficiency and net-work generation.*
The products composition was determined by applying the Gibbs-minimization method together with mass and energy conservation equations. On the other hand, the detonation temperature and the products composition after the detonation process were determined by applying the Chapman-Jouguet theory together with Gibbs-minimization, mass conservation and energy conservation equations. The results obtained show that the detonation-chamber-based turbine wields a higher thermal efficiency than the combustion-chamber-based turbine in all comparisons made utilizing equal initial parameters; however, the pressure and temperature of the chemical products in the detonation chamber are significantly higher, which, although theoretically beneficial, showcase practical limitations that imply the need of adaptations in the form of modifying the pre-and-post-combustion parameters and process in the thermodynamic energy generation process.

Keywords: *Detonation engine, combustion reaction, gas turbine, thermodynamic cycle*

1. INTRODUCTION

The gas turbines operating with combustion chambers at constant pressure are internal combustion engines extensively used in various fields of application, notably in the propulsion of aircraft, but also in the propulsion of ships and tanks and as electrical generators, pumps, and compressors (BORGNAKKE; SONNTAG, VAN WYLEN, 2002). Fuel combustion in gas turbines occurs in the combustion chamber. Turns (2011) develops a model where a combustion reaction occurs at constant pressure between air and fuel, resulting in combustion product gases.

Because they are so relevant in these fields, there is a high interest to improve the thermal efficiency of gas turbines; however, current conventional turbines have thermal efficiency very close to the theoretical ideal (LI *et al.*, 2018). Turbines operating with Rotating Detonation Engines (RDE) are an alternative technology to conventional turbines. In this type of turbine, the combustion chamber is a detonation chamber, where the speed of the products is supersonic. Reagents are fed through an annular cylindrical chamber and a detonation wave travels around the chamber in an helicoidal pattern. Continuous detonation is initiated only one time and operates at typical frequencies of 1-10Hz (BATTELLE, 2017). RDEs are a promising innovation because with them it is possible to obtain higher thermal efficiencies compared to turbines operating with conventional combustion chambers (WOLAŃSKI, 2017).

Naples and Hoke (2017) developed a rotating detonation engine and coupled the RDE with a T63 gas turbine. The RDE runs multiple power settings and demonstrates turbine performance equivalent to or better than the stock combustor using hydrogen fuel. Their results show that high frequency, 25% unsteady temporal pressure at a combustor outlet is not detrimental to uncooled turbine performance, and may even increase turbine efficiency. Numerical simulations were

performed by Yao *et al.* (2017) to RDEs with a hollow chamber, based on the reactive Euler equations and one-step Arrhenius chemistry model. The fuel injection area ratios range from 55.6% to 88.9% and the propulsive performance of the hollow RDE with different fuel injection area ratios is also evaluated and compared with experimental data and other simulation results.

Bigler *et al.* (2017) realized a comparative study between ideal thermodynamic cycles representing conventional gas turbines (using the Brayton cycle) and turbines with RDEs, using air as the working fluid; the detonation cycle presented a higher thermal efficiency as a function of all analyzed parameters. A comparation of the performance of a conventional Brayton cycle with a subsonic turbine and a detonation cycle with a supersonic turbine was realized by Sousa et al. (2017), through different compression ratios. The detonation cycle has a relative thermal efficiency gain of more than 6.7% for equal compression ratios.

Bluemmer *et al.* (2019) performed an experimental study on the transition dynamics in a hydrogen-air rotating detonation combustors RDC as the operating mode transitions from two steadily propagating, equally-fast counter-rotating waves to a single wave depending on the operating condition. Their results indicate a correlation between the operating mode with two counter-rotating waves and choked flames, as well as quasi-detonations observed in generic detonation experiments in the literature. The work of Dai et al. (2019) develops a thermodynamic cycle where there is an extraction flow in the compressor, at 50% of the final pressure, which feeds the detonation chamber; the remaining air cools the product gases in a dilution process. A study about the effect of different K_2CO_3 ionized seed mass contents on the detonation process was realized by Lin *et al.* (2020). The PDE was successfully ignited and formed a stable detonation wave at ignition frequencies of 5 Hz and 10 Hz, and the peak pressure of the stable detonation with the ignition frequency of 5 Hz was 17% higher than that with an ignition frequency of 10 Hz.

The main objective of this work is to carry out a comparison between a thermodynamic cycle representing a conventional gas turbine, with a combustion chamber at constant pressure, and a thermodynamic cycle representing a turbine operating with an RDE, that is, with a detonation chamber. The parameters compared are the work supplied to the compressor, the work supplied by the turbine and principally the thermal efficiency of the cycle; these parameters are compared across a range of different compression ratios. Mathematical and computational models were developed to represent these two cycles operating in steady state and considering that the combustion and detonation processes reach equilibrium. The combustion products are mixed with air in a dilution process at constant pressure.

2. METHODOLOGY

The constant-pressure combustion thermodynamical cycle and the detonation cycle considered are shown, respectively, in the Figures 1 and 2. The cycles are compared across compression ratios, r, varying from 4 to 40. In the detonation cycle, air is extracted from the compressor in an intermediate pressure p_I; the ratio between p_I and the outlet pressure of the compressor p_1 is called the pressure fraction f. Three cases were considered for the detonation cycle, with values of f equal to 0,3, 0,5 and 0,7, respectively.

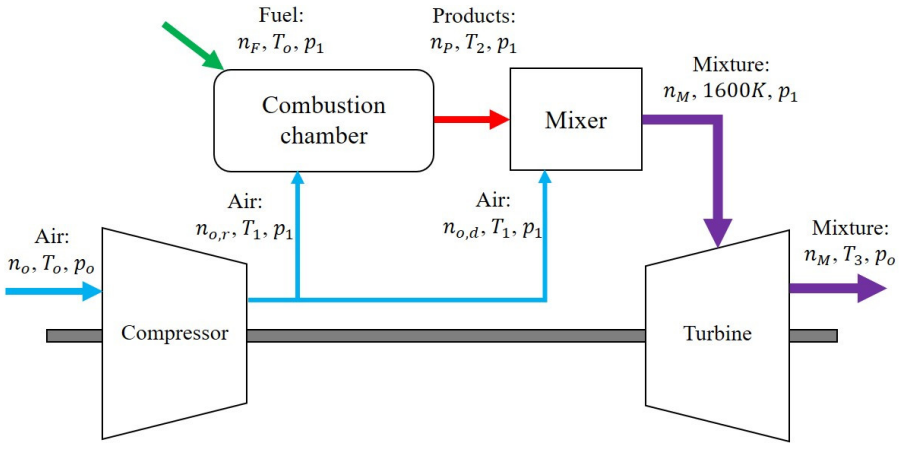

Figure 1. Scheme of the constant-pressure combustion thermodynamic cycle.

It is considered that the combustion is stoichiometric, being the reference pressure and temperature equal to 100.000 Pa and temperature 298,15 K, respectively (IUPAC, 1982). The global combustion reaction considered is shown in the Eq. (1).

$$C_{x_C}H_{x_H}O_{x_O}N_{x_N} + \nu_{ar}^{s}\,(O_2 + 3{,}76N_2) \rightarrow n_{CO_2}CO_2 + n_{CO}CO + n_{H_2O}H_2O + n_{H_2}H_2 + n_{O_2}O_2 + n_{N_2}N_2 \quad (1)$$

where n_i is the mol number of the chemical species i, and ν_{ar}^{s} is the air coefficient of the reaction. The species in the products are H_2O, CO_2, N_2, O_2, H_2 and CO, the presence of H2 and CO denotes the possibility of incomplete combustion. The composition of the products is determined by applying the method of minimization of Gibbs free energy.

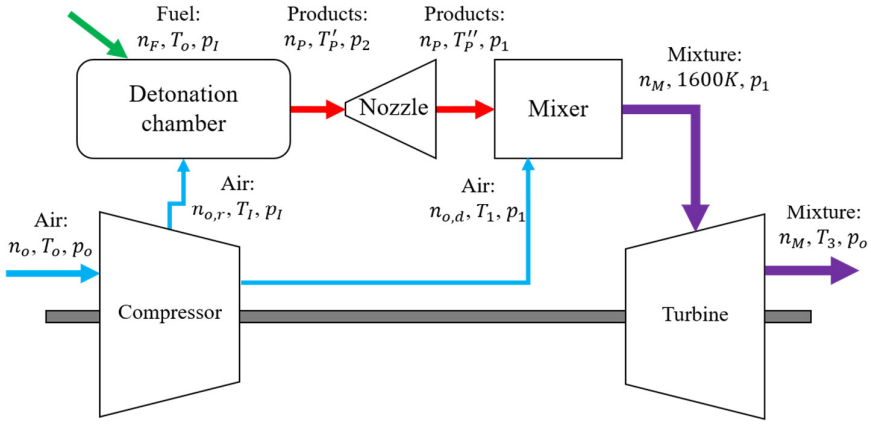

Figure 2. Scheme of the detonation thermodynamic cycle.

Considering the different equipment that form the cycle, the work done in the compressor W_C, in J, is determined by the Eq. (2).

$$W_C = n_o.\left(\bar{h}_I - \bar{h}_o\right) + n_{o,d}.\left(\bar{h}_1 - \bar{h}_I\right) \tag{1}$$

where n_o is total quantity of air which enters the compressor and $n_{o,d}$ is the quantity of air which goes to the mixer, called the dilution air, both in mol. $\bar{h}_o$, $\bar{h}_I$ and $\bar{h}_1$are, respectively, the molar enthalpies of the air in the initial, intermediary and final states of the compression process, in J/mol; in the constant-pressure combustion cycle, there is no extraction air, so $\bar{h}_I = \bar{h}_1$. The molar enthalpies, as well as all other thermodynamical proprieties considered in this paper, are determined computationally utilizing the NASA-Glenn polynomials and coefficients (Gordon *et al.*, 2002). The air in the inlet is considered at the standard temperature and pressures of 293.15 K and 103 325 Pa and is composed of 21% of O_2 and 79% of N_2. n_o equals the sum of the quantity of dilution air $n_{o,d}$ with the quantity of reaction air $n_{o,r}$[mol]. The quantity of reaction air is given by Eq. (3).

$$n_{o,r} = 4{,}76.\nu_{ar}^{s} \tag{3}$$

The isentropic efficiency η_C of the compressor is considered equal to 0,85. Equations (4) and (5) relate the isentropic efficiency with, respectively, the isentropic molar enthalpy of the intermediate state $\bar{h}_{Is}$ and final state $\bar{h}_{1s}$ of the air and its real analogues, $\bar{h}_I$ and $\bar{h}_1$, and the molar enthalpy of the initial state $\bar{h}_o$, all in J/mol.

$$\eta_C = \frac{\bar{h}_{Is} - \bar{h}_o}{\bar{h}_I - \bar{h}_o} \tag{4}$$

$$\eta_C = \frac{\bar{h}_{1s} - \bar{h}_o}{\bar{h}_1 - \bar{h}_o} \tag{5}$$

Equations (6) and (7) describe the isentropic compression processes from the initial state to the intermediary and final states, respectively.

$$\bar{s}_{1s}^{o} = \bar{s}_o^{o} + \bar{R}.ln\frac{p_1}{p_o} \tag{6}$$

$$\bar{s}_{Is}^{o} = \bar{s}_o^{o} + \bar{R}.ln\frac{p_I}{p_o} \tag{7}$$

where $\bar{s}_o^o$, $\bar{s}_{ls}^o$ and $\bar{s}_{1s}^o$ are, in this order, the molar entropies of the air in the initial state, in the intermediary isentropic state, and the final isentropic state, all in J/mol-K. $\bar{R}$ is the gas constant, equal to 8,134 J/mol-K. In the constant-pressure combustion chamber, the energy conservation is given by Eq. (8)

$$H_P = H_R \tag{8}$$

where H_P and H_R are, respectively, the total enthalpies of the products and the reactants, in J, given by the sum of the enthalpies of each of its component species. The products are at equilibrium, at an adiabatic flame temperature T_{ad}. In the detonation chamber the Chapman-Joguet theory is applied, given by the system of equations shown in Eqs. (9) to (11).

$$\dot{m}'' = \rho_P . u_P = \rho_R . u_R \tag{9}$$

$$p_P + \rho_P . u_P^2 = p_R + \rho_R . u_R^2 \tag{10}$$

$$h_P + \frac{u_P^2}{2} = h_R + \frac{u_R^2}{2} \tag{11}$$

where $\dot{m}''$ is the mass flux, in kg/m².s; ρ_P and ρ_R are the specific masses of the products and reactants as a whole, in kg/m³; u_P and u_R are the velocities of the products and the reactants, in m/s; and h_P and h_R are the specific enthalpies of the products and reactants as a whole, in J/kg.

In the detonation cycle, the combustion products pass through a nozzle before entering the mixer, where their pressure is reduced from the detonation pressure until it equals the pressure of the dilution air. Equation (12) relates the stagnation temperature T_e, in K, with the temperature T, also in K, in an arbitrary point in the nozzle. k is the thermal capacity ratio and M is Mach number of the combustion products in this arbitrary point.

$$\frac{T}{T_e} = 1 + \frac{k-1}{2} M^2 \tag{12}$$

Equation (13) relates the stagnation pressure p_e, in Pa, with the pressure p, also in Pa, in an arbitrary point in the nozzle.

$$\frac{p}{p_e} = (1 + \frac{k-1}{2} M^2)^{\frac{k}{k-1}} \tag{13}$$

The product gases of the combustion go through the mixer where they are diluted with compressed air which got through the total compression process in the compressor. The temperature of the mixture of air and combustion products is considered equal to 1600 K, the upper limit of the range in which commercial turbines can safely operate (De Souza, 2014). The quantity of air needed to cool the product gases to 1600 K is given by the Eq. (14)

$$n_{o,d} = \frac{n_P(\bar{h}_{P,2} - \bar{h}_{P,1})}{(\bar{h}_{o,d,2} - \bar{h}_{o,d,1})} \tag{14}$$

where n_P is the quantity of the combustion products, in mol; $\bar{h}_{P,1}$ and $\bar{h}_{P,2}$ are the molar enthalpies of the product gases in the inlet and outlet of the mixer, respectively, in J/mol; and $\bar{h}_{o,d,1}$ and $\bar{h}_{o,d,2}$ are the molar enthalpies of dilution air in the inlet and outlet of the mixer, respectively, in J/mol. The air-products mixture enters the turbine, realizing an expansion work W_T, in J, given by the Eq. (15)

$$W_T = n_M . (\bar{h}_3 - \bar{h}_2) \tag{15}$$

where n_M is the quantity of mixture, in mol, and $\bar{h}_2$ and $\bar{h}_3$ are the molar enthalpies of the mixture in the inlet and outlet of the turbine, respectively, in J/mol. The isentropic efficiency η_T of the turbine is considered equal to 0,9. Equation (16) relates the isentropic efficiency with the isentropic molar enthalpy of the mixture in the outlet $\bar{h}_{3s}$ and its real analogue $\bar{h}_3$, as well as its inlet state $\bar{h}_2$, all in J/mol.

$$\eta_T = \frac{\bar{h}_2 - \bar{h}_3}{\bar{h}_2 - \bar{h}_{3s}} \tag{16}$$

Equation (17) describes the isentropic expansion processes from the inlet state to the outlet state. The inlet pressure is equal to the outlet pressure of the compressor p_1. The outlet pressure is equal to the atmospheric pressure p_o.

$$\bar{s}_{3s}^{o} = \bar{s}_{2}^{o} + \bar{R}.ln\frac{p_1}{p_2} \tag{17}$$

The thermal efficiency of the cycle is given by Eq. (18).

$$\eta = \frac{W_T - W_C}{n_F.\overline{LHW}} \tag{18}$$

where n_F is the quantity of fuel, in mol, equal to 1. The molar lower heating value of the fuel, $\overline{LHW}$, is calculated via the Eq. (19)

$$\overline{LHW} = \frac{H_R - H_P}{n_F} = \sum_{r}^{R} n_r.\bar{h}_r^o - \sum_{p}^{P} n_p.\bar{h}_p^o \tag{19}$$

where the summations represent the sum of the molar enthalpies $\bar{h}_r^o$ and . $\bar{h}_p^o$, in J/mol, of each component species of the reactants and products, respectively, in the reference state, multiplied by its respective quantity n_r or n_p, in mol. In this paper, the fuel considered is a synthesis gas obtained via gasification of biomass and residues (Babu, 2013). The composition of the synthesis gas is shown in Table 1.

Table 1. Composition of the fuel in mole fractions.

Chemical species	Mole fraction
Carbon monoxide (CO)	0.48
Hydrogen (H_2)	0.32
Carbon dioxide (CO_2)	0.15
Nitrogen (N_2)	0.03
Methane (CH_4)	0.02

The synthesis gas yields a $\overline{LHW}$ of 229 284.78 J/mol and has a molar formation enthalpy at the reference state $\bar{h}_F^o$ of -113 568.72 J/mol. The air coefficient v_{ar}^s is equal to 0.44 and the quantity of reaction air $n_{o,r}$ is equal to 2.0944 mol.

3. RESULTS AND DISCUSSIONS

The results obtained using the computational models, pertaining to the thermal efficiency and the total work to the compressor and from the turbine, in each case, are presented and commented in the following sub-sections.

3.1. Work done in the compressor

The work needed by the compressor is similar between the three analyzed cases of the detonation cycle, as shown in the Figure 3. For the same compression ratio, the larger the pressure fraction, the larger is the fraction of the total work needed for the compression of the reaction air; although, due the lower temperature of the combustion products at the outlet of the nozzle (as shown in the Table 2), this effect is compensated by the smaller quantity of dilution air needed to cool the product gases to 1600 K.

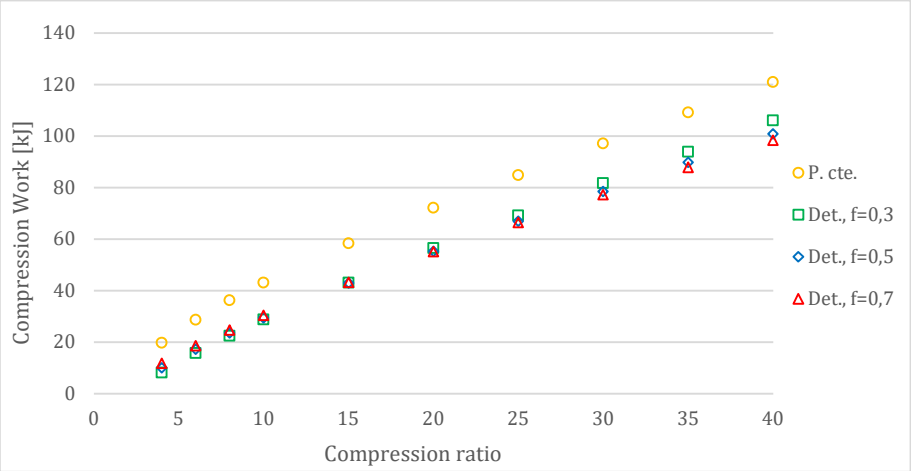

Figure 3. Work done in the compressor for constant-pressure combustion cycle (P.cte) and detonation cycle for three different pressure fractions ($f = 0{,}3$, $f = 0{,}5$ and $f = 0{,}7$) as a function of the compression ratio.

Table 2. Inlet turbine temperature [K]; for the constant-pressure combustion, equal to the adiabatic flame temperature; for the detonation, equal to the outlet nozzle temperature.

r	**4**	**6**	**8**	**10**	**15**	**20**	**25**	**30**	**35**	**40**
p = const.	2202.2	2237.8	2265.4	2288.3	2333.1	2367.0	2396.3	2420.8	2442.4	2461.7
f = 0.3	2059.2	2129.4	2180.7	2221.4	2297.4	2353.2	2397.6	2434.7	2466.5	2494.6
f = 0.5	1952.7	2019.6	2068.6	2107.5	2180.3	2234	2276.7	2312.7	2343.2	2370.3
f = 0.7	1886.0	1950.8	1998.4	2036.3	2107.3	2159.5	2201.3	2236.2	2266.3	2292.9

The work done in the compressor in the constant-pressure combustion cycle is significantly larger in comparison with the detonation cycle. That occurs for two reasons: first, for an equal compression ratio r, all the air that enters the compressor in the constant-pressure cycle is compressed at this ratio, in contrast with the detonation cycle, where only the dilution air is compressed at r, with the rest being compressed just at r_1; second, the inlet temperatures of the combustion products in the mixer are larger in the constant-pressure cycle because there was no nozzle considered in that case.

3.2. Work done by the turbine

The inlet temperature and pressure and the outlet pressure in the turbine are always the same in all the considered scenarios; the only variable parameters, that influence the enthalpy difference between the outlet and inlet of the turbine, are the quantity and composition of the product gases, the quantity of dilution air and the outlet temperature of the air-products mixture.

The fraction of the total work performed by the expansion of the combustion gases is a negligible factor in the case-by-case comparison, due to its quantity and composition being approximately the same in all cases studied in the present work. The outlet temperature of the mixture is also a negligible factor in the analysis. The turbine outlet temperature is shown in the Table 3 for different compression ratios and intermediate pressures.

Table 3. Outlet turbine temperature [K].

r	**4**	**6**	**8**	**10**	**15**	**20**	**25**	**30**	**35**	**40**
p = const.	1225.2	1132.3	1070.1	1023.8	944.0	890.6	850.9	819.6	793.8	772.1
f = 0.3	1226.3	1132.7	1069.9	1023.2	942.6	888.6	848.6	817.1	791.2	769.4
f = 0.5	1229.3	1136.1	1073.5	1026.8	946.2	892.2	852.1	820.5	794.5	772.6
f = 0.7	1231.5	1138.5	1076.0	1029.4	948.8	894.7	854.6	822.8	796.8	774.8

It is observed that for larger pressure fractions in the detonation cycle, the outlet temperature in the outlet of nozzle is lower. Therefore, a smaller quantity of dilution air is needed for the cooling process, consequently, diminishing the work done by the turbine. The turbine work in the detonation cycle in most cases is smaller than the turbine work in the constant-pressure cycle, as shown in the Figure 4, except for f = 0,3. In that case, the work is larger for compression ratios larger than 25, the inlet temperature in the mixer surpasses its equivalent in the constant-pressure cycle, being need a larger quantity of dilution air.

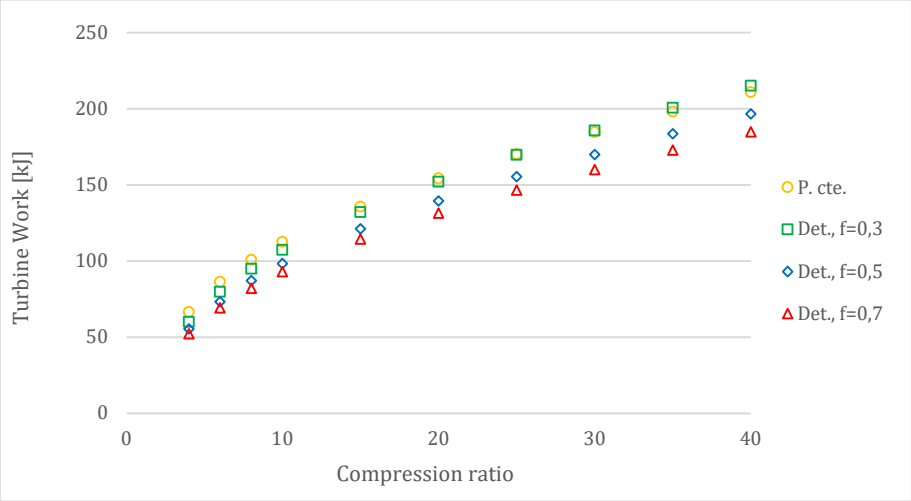

Figure 4. Work done by the turbine for constant-pressure combustion cycle (P.cte) and detonation cycle for three different pressure fractions ($f = 0{,}3$, $f = 0{,}5$ and $f = 0{,}7$) as a function of the compression ratio.

3.3. Thermal efficiency

The thermal efficiency curves of the three analyzed detonation cycles behave similarly when compared with each other. However, the largest thermal efficiency was obtained for the case of the pressure fraction equal to 0,3, as shown in the Figure 5. The Figure also contains the thermal efficiency of cycle gas turbines of fabricant Mitsubishi Hitachi Power Systems, tested with natural gas for different pressure ratios. These values can be compared with the thermal efficiency of constant-pressure combustion cycle calculated by the developed model. The specifications of these gas turbines can be founded in Table 4. Was not found data for detonation cycles with similar operating conditions to those studied in this work. It can be observed that for compressions ratios between 14 and 23 the experimental thermal efficiency of Mitsubishi Hitachi Gas Turbines falls between 34.9 and 41.0 %, this is in accordance with the results obtained with the model developed in the present work, which determined thermal efficiencies among 33.9 and 35.9% for compression ratios between 20 and 25. The difference in thermal efficiencies can be explained by higher concentration of inert gases in the syngas used for the simulations performed in this work.

Table 4. Thermal efficiencies of simple cycle gas turbines of fabricant Mitsubishi Hitachi Power Systems tested with natural gas (Gas Turbine World, 2014).

Model	Power (MW)	Mass flow rate (kg/s)	Compression Ratio	Thermal Efficiency (%)	Heat rate (kJ/kWh)
M501DA	113.9	346.1	14.0	34.9	10318.4
M501F3	185.4	458.6	16.0	37.0	9738.1
H-80	110.6	307.2	19.2	37.6	9584.1
M501G1	267.5	598.8	20.0	39.1	9210.7
M501J	327.0	598.8	23.0	41.0	8783.3

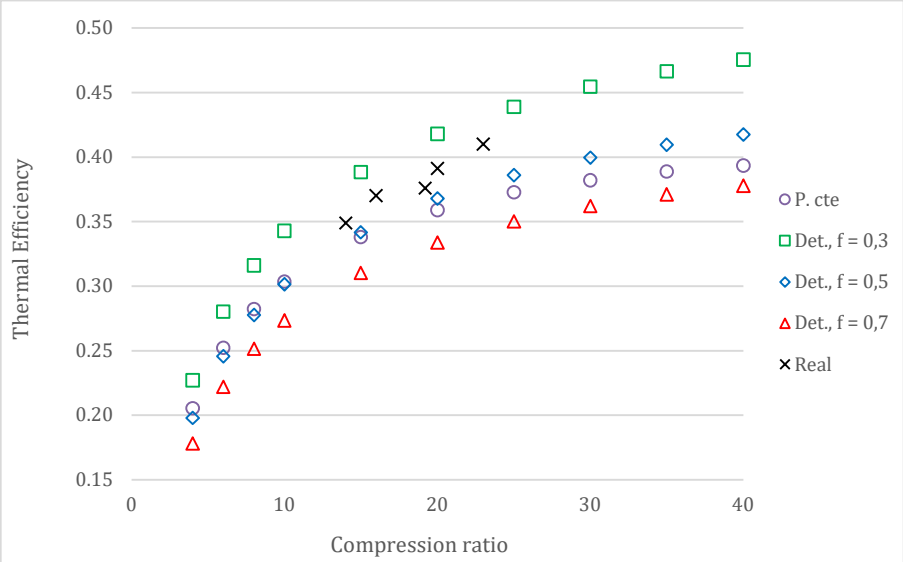

Figure 5. Thermal efficiency for constant-pressure combustion cycle (P.cte), detonation cycle for three different pressure fractions ($f = 0{,}3$, $f = 0{,}5$ and $f = 0{,}7$) and for Mitsubishi Hitachi Power Systems gas turbines (real) as a function of the compression ratio.

When compared to the constant-pressure combustion cycle, only the detonation cycle at $f = 0.3$ possesses a larger thermal efficiency for all the values of r considered in the analysis. At $f = 0.5$, the thermal efficiency surpasses the constant-pressure cycle only for compression ratios larger than 10, approximately. The thermal efficiency of the detonation cycle at $f = 0.7$ is smaller than the constant-pressure cycle for all pressure ratios considered. Table 5 shows the relative gains of the detonation cycles in comparison with the constant-pressure combustion cycle.

The thermal efficiency curves of the detonation cycles grow faster, with the increase of r, than the curve of the constant-pressure cycle. Therefore, it is possible to infer that the termal efficiency of the detonation cycle at $f = 0.7$ outgrows the constant-pressure cycle for compression ratios larger than 40; only further simulations can confirm this hypothesis, tough. However, the fact that a lower compression, $f = 0.3$, is enough to surpass the efficiency of the constant-pressure cycle is an important result which shows the advantage of the detonation cycle, since there is an increase in pressure inside the detonation chamber.

Table 5. Relative gains in thermal efficiency of the detonation cycles compared to the constant-pressure combustion cycle.

r	**4**	**6**	**8**	**10**	**15**	**20**	**25**	**30**	**35**	**40**
$f = 0.3$	10.63%	11.09%	12.00%	12.90%	14.87%	16.46%	17.79%	18.94%	19.96%	20.90%
$f = 0.5$	-3.55%	-2.60%	-1.59%	-0.70%	1.10%	2.48%	3.59%	4.56%	5.36%	6.11%
$f = 0.7$	-13.29%	-11.95%	-10.85%	-9.95%	-8.24%	-7.01%	-6.04%	-5.23%	-4.55%	-3.94%

Due to the detonation cycle using a supersonic turbine, the kinetic energy variation can be a significant component in the energy balance of the turbine. In future works, the kinetic energy variation should be considered, with a dynamic analysis of the turbine being needed; this is beyond the scope of the present work. It can be inferred, although, that the thermal efficiency of the detonation cycle should be higher for every pressure fraction f if the kinetic energy variation was considered.

4. CONCLUSIONS

The comparison between the results obtained with the thermodynamic models for the gas turbine working with a constant-pressure combustion chamber and with a detonation combustion chamber, shows the increase of the thermal efficiency for low extraction pressure ratios (*f=0.3*). In general, the thermal efficiency of the detonation cycle decreases with increasing extraction pressure ratios.

The constant-pressure cycle presents a higher compression work than the detonation cycle. However, the work performed by the turbine, for the constant-pressure cycle, is slightly higher than that performed with the detonation cycle.

The work performed by the turbine increases as the extraction pressure ratio is lower (*f=0.3*). In the case of *f=0.3*, the relative gain in thermal efficiency increases with the compression ratio from 10.63% at *r=4* to 20.90% for *r=40*.

In future works, the strategy for lowering the temperature of the products leaving the detonation chamber can also be considered as a variable parameter. It is also possible to show the variation of the thermal efficiency by changing the turbine inlet temperature, which was considered constant, and equal to 1600K in the present work. Future work can also consider more complex cycle in order to obtain further increases in the thermal efficiency.

5. REFERENCES

Basu, Prabir, and Biomass Gasification, 2017. "Pyrolysis and Torrefaction Practical Design and Theory." (2013).

Naples, Andrew, et al. "RDE implementation into an open-loop T63 gas turbine engine." *55th AIAA Aerospace Sciences Meeting*.

Bigler, Blaine R., Eric J. Paulson, and William A. Hargus, 2017. "Idealized efficiency calculations for rotating detonation engine rocket applications." *53rd AIAA/SAE/ASEE Joint Propulsion Conference*.

Bluemner, R., et al, 2019. "Counter-rotating wave mode transition dynamics in an RDC." *International Journal of Hydrogen Energy* 44.14: 7628-7641.

Borgnakke, C.; Sonntag, R.E.; Van Wylen, G. J., 2002. "Fundamentos da Termodinâmica: Tradução da 5ª edição americana". *São Paulo: Edgard Blücher*.

CARVALHO JR., J. A. et al., 2018. "Combustão aplicada". 1. ed. *Florianópolis: EdUFSC.*

Shapiro, Howard N., and Michael J. Moran, 2009. "Princípios de termodinâmica para engenharia." *LTC,* Ed 6.

Qi, Lei, et al., 2019. "Investigation of the pressure gain characteristics and cycle performance in gas turbines based on interstage bleeding rotating detonation combustion." *Entropy* 21.3: 265.

DAI, Y. et al., 2019. "Investigation of the Pressure Gain Characteristics and Cycle Performance in Gas Turbines Based on Interstage Bleeding Detonation Combustion." *Applied Mechanics and Materials, [s. l.], v. 782, p. 3–12*.

De Souza, Z., 2014 "Plantas de Geração Térmica a Gás: Turbina a Gás, Turbocompressor, Recuperador de Calor, Câmara de Combustão." *1. ed. Rio de Janeiro: Interciência*.

Fox, Robert W., Philip J. Pritchard, and Alan T. McDonald, 2000. "Introdução à Mecânica Dos Fluidos*". Grupo Gen-LTC.*

Gas Turbine World, 2014 Performance Specs, *Vol. 44, No. 1, January–February 2014, Pequot Publis- hing, 2014.*

Gordon, S.; McBride, B. J.; Zehe, M. J., 2002. "NASA Glenn Coefficients for Calculating Thermodynamic Properties of Individual Species." *Washington D.C.: NASA*.

IUPAC, 1982. "Notation for states and processes, significance of the word standard in chemical thermodynamics, and remarks on commonly tabulated forms of thermodynamic functions." *Pure & Applied Chemistry, [s. l.], v. 54, n. 6, p. 1239–1250.*

LEE, J. H. S.*,* 2008. "The Detonation Phenomenon." *1. ed. Cambridge: Cambridge University Press*.

Li, Z. et al., 2018. "A Thermodynamic Analysis of the Pressure Gain of Continuously Rotating Detonation Combustor for Gas Turbine." *Applied Sciences, [s. l.], v. 8, n. 4, p. 535–553*.

Lin, Ling, et al., 2020. "Experimental study on the detonation process of a pulse detonation engine with ionized seeds." *Defence Technology* 16 :178-187.

Sousa, Jorge, Guillermo Paniagua, and Elena Collado Morata, 2017. "Thermodynamic analysis of a gas turbine engine with a rotating detonation combustor." *Applied energy* 195: 247-256.

Morata, Elena C.; Panaigua, Guillermo; Sousa, Jorge*,* 2017. "Thermodynamic analysis of a gas turbine engine with a rotating detonation combustor." *Applied Energy, [s. l.], v. 195, p. 247–256*.

NIST. JANAF, 1971. "Thermochemical Tables. 2. ed*. Gaithersburg: National Bureau of Standards*.

Saad, M. A*,* 1992. "Compressible Fluid Flow." *2.* ed*. Hoboken: Prentice Hall*.

Turns, S, 2012. "An Introduction to Combustion**:** Concepts and Applications." 3. ed*. New York: McGraw-Hill*.

Wolański, Piotr, 2015. "Application of the continuous rotating detonation to gas turbine." *Applied Mechanics and Materials*. Vol. 782. Trans Tech Publications Ltd.

Yao, Songbai, et al, 2017. "Numerical study of hollow rotating detonation engine with different fuel injection area ratios." *Proceedings of the Combustion Institute* 36.2:2649-2655.

6. RESPONSIBILITY NOTICE

The author(s) is (are) the only responsible for the printed material included in this paper.